Fixed-Time Formation Tracking for Heterogeneous Linear Multiagent Systems With a Nonautonomous Leader

Shiyu Zhou, *Graduate Student Member, IEEE*, Dong Sun, *Fellow, IEEE*, and Gang Feng, *Fellow, IEEE*

***Abstract*—This article studies the fixed-time time-varying formation (TVF) tracking control problem for heterogeneous multiagent systems with a nonautonomous leader under a directed communication network. The primary objective is to design a TVF tracking protocol enabling the followers to form the desired TVF while simultaneously tracking the output of the nonautonomous leader in a fixed time. First, a distributed fixed-time observer is proposed to estimate the state of the nonautonomous leader under a directed communication network. Then, utilizing coordinate transformation and sliding mode techniques, a fixed-time observer-based TVF tracking protocol is developed without requiring the full row rank assumption on the input matrix of the follower. It is proved via the Lyapunov stability theory that the fixed-time TVF tracking problem with a nonautonomous leader can be solved under the proposed protocol. Finally, the effectiveness of the proposed fixed-time TVF tracking control protocol is demonstrated by numerical examples.**

***Index Terms*—Cooperative output regulation, directed graph, fixed-time control, heterogeneous linear multiagent systems (MASs), time-varying formation (TVF) tracking.**

I. Introduction

FORMATION control of multiagent systems (MASs) has attracted considerable attention in recent decades, owing to its widespread applications across a range of fields, for instance, networked robot systems [1], [2], [3], [4]; multiple spacecraft systems [5], [6], [7]; and satellite systems [8], [9], [10]. Different formation control approaches, encompassing behavior-based, leader-follower-based, virtual structure-based, and consensus-based methods, have been developed, with the last one being a more general approach that encompasses the former three [11]. In fact, consensus-based formation control strategies have become more and more popular due to their advantages of less computational and communication costs, stronger robustness against faults and attacks, and also better scalability, especially for large-scale MASs [12], [13], [14], [15], [16].

In many practical applications, apart from realizing the specific formation, it is also often desirable for the MAS to track certain given trajectories. This is the so-called formation tracking problem, and it has garnered significant interest in the past few years, see, for instance, [17], [18], and [19]. In [18], a distributed formation strategy for the arbitrary number of leaders was developed. The consensus-based time-varying formation (TVF) tracking problem for multiple leaders was investigated in [19]. It should be pointed out that agent dynamics in the aforementioned studies are assumed to be homogeneous. In many tasks, such as forest fire monitoring that involves the use of both autonomous aerial vehicles (AAVs) and autonomous ground vehicles (AGVs), it is critical to take into account different agent dynamics, which are commonly referred to as heterogeneous multiagent systems (HMASs). Indeed several recent studies have investigated the problem of formation tracking for HMASs using the celebrated cooperative output regulation theory [20], [21], [22], [23], [24]. Yaghmaie et al. [20] investigated the multiparty output consensus problem of HMASs and demonstrated the effectiveness of their proposed method by applying it to TVF tracking. The TVF tracking control protocols have been proposed for HMASs in [21] with an autonomous leader and in [22], [23], and [24] with nonautonomous leaders, respectively.

It is worth noting that the aforementioned studies [20], [21], [22], [23], [24] primarily concentrate on the asymptotic convergence of the concerned MASs. This means that the goal of cooperative control of MASs can be achieved only when time goes to infinity. However, in practice, it is often desirable to achieve the goal of cooperative control for MASs in a finite time [25], [26], [27], [28], [29] as finite-time convergence often implies fast convergence and better robustness. Thus, finite-time formation tracking problems have received extensive attention in recent years, see, for example [30], [31], [32], and [33]. However, those finite-time formation tracking control methods, such as those finite-control of single systems [25], [26], [27], [28], [29], suffer a drawback, that is, the upper bounds of their finite-time convergence are dependent on the initial states of the concerned systems and could be very large if the initial states are far away from their equilibrium. Inspired by Polyakov's [34] work on the fixed-time stability where the upper bound of the convergence time is independent of initial conditions,

Received 8 August 2024; revised 4 November 2024; accepted 8 November 2024. Date of publication 10 January 2025; date of current version 20 June 2025. This work was supported by the Research Grants Council of Hong Kong under project CityU-11205024. Recommended by Associate Editor H.-S. Ahn. *(Corresponding author: Gang Feng.)*

The authors are with the Department of Biomedical Engineering, City University of Hong Kong, Kowloon, Hong Kong (e-mail: shiyuzhou9-c@my.cityu.edu.hk; medsun@cityu.edu.hk; megfeng@cityu.edu.hk).

Digital Object Identifier 10.1109/TCNS.2025.3528095

2325-5870 © 2025 IEEE. All rights reserved, including rights for text and data mining, and training of artificial intelligence and similar technologies. Personal use is permitted, but republication/redistribution requires IEEE permission. See https://www.ieee.org/publications/rights/index.html for more information.

Authorized licensed use limited to: Hong Kong Polytechnic University. Downloaded on September 15,2025 at 15:32:38 UTC from IEEE Xplore. Restrictions apply.

some results on fixed-time cooperative control of MASs have been reported [35], [36], [37], [38], [39], [40], [41]. Fixed-time consensus algorithms for MASs with integrator-types dynamics were developed in [35] and [36]. Fixed-time TVF tracking control problems of HMASs were studied in [39] with an autonomous exosystem and in [40] and [41] with a nonautonomous exosystem, respectively. However, those approaches developed in [40], [39], and [41] are based on two key assumptions: the communication graphs among agents are undirected, and the input matrices of follower agents must be of full row rank, both of which could be too restrictive in practical application and thus not desirable. It can be observed from the above literature review that the problem of fixed-time TVF tracking for HMASs with a nonautonomous leader has yet been addressed, which motivates this study.

This article investigates the fixed-time TVF tracking problem for HMASs with a nonautonomous leader under a directed communication network. The coexistence of an asymmetric Laplacian matrix and the command input of the nonautonomous leader significantly complicates the protocol design and stability analysis. To this end, we first propose a distributed observer to estimate the nonautonomous exosystem under a directed graph. Then, an observer-based control protocol is proposed that does not require the generalized inverse matrix of the input matrix of the follower. Compared with those existing relevant works, this work has the following main contributions.

1) A novel distributed fixed-time control protocol consisting of distributed fixed-time observers and fixed-time controllers is developed. The distributed observers are designed to estimate the state of the nonautonomous leader under a directed communication network. Based on the distributed observer, integral sliding mode-based controllers are put forward so that the fixed-time TVF tracking problem is solved. Unlike those works [21], [22], and [23] with asymptotic convergence, and [30], [31], [32], and [33] with finite-time convergence, this work achieves fixed-time TVF tracking control with an explicit finite upper bound on the settling time that is independent of the initial states of the concerned HMAS.
2) Unlike the fixed-time control methods described in [39], [40], and [41], where the input matrix of the follower is implicitly assumed to be of full row rank, our fixed-time TVF tracking protocol is developed using coordinate transformation and sliding mode techniques, thereby eliminating the need for this restrictive assumption.
3) In contrast to [35], [36], [37], [38], [39], [40], and [41] where undirected and connected graphs are considered, this work considers more general directed communication graphs. Given that the Laplacian matrix of directed graphs is asymmetric, the design of fixed-time protocols and the stability analysis become more challenging compared to their counterparts in undirected networks. Moreover, directed communication networks are more common in practical MASs, and thus, the proposed TVF tracking protocol is expected to have wider applications in practice.

Notations: $\mathbf{1}_M$ and $\mathbf{0}_M$ are the $M \times 1$ vectors with all elements being 1 and 0, respectively. The n-dimensional identity matrix is denoted as I_n. $\otimes$ represents the Kronecker product. The diagonal matrix is denoted as $\mathrm{diag}\{a_1, \ldots, a_n\}$ with a_i, $i = 1, \ldots, n$, as its diagonal entries. For a vector $\mathcal{Q} = [q_1, \ldots, q_n]^\top \in \mathbb{R}^n$, $\|\mathcal{Q}\|_p \triangleq (\sum_{i=1}^n |q_i|^p)^{\frac{1}{p}}$ with $p > 0$ and $\|\mathcal{Q}\|$ denotes its Euclidean norm. Denote $\mathrm{sig}^\mu(\mathcal{Q}) = [\mathrm{sign}(q_1)|q_1|^\mu, \ldots, \mathrm{sign}(q_n)|q_n|^\mu]^\top$, where $\mu > 0$ and $\mathrm{sign}(\cdot)$ represents the sign function. Let $\|\cdot\|_\infty$ be the $\mathcal{L}$-infinity norm. $\min(\cdot)$ and $\max(\cdot)$ are used to determine the minimum and maximum elements of an array, respectively.

II. Preliminaries and Problem Formulation

A. Algebraic Graph Theory

This article considers a HMAS consisting of M followers and one leader. An agent is defined as a leader if it has no neighbors, while it is designated as a follower if it is connected to at least one other agent. The set of the followers is defined as $\mathcal{O}_f \triangleq \{1, \ldots, M\}$. Let $\mathcal{G}_F = (\mathcal{O}_f, \mathcal{E}_f, \mathcal{W}_f)$ represent the digraph among followers, which consists of the set of nodes $\mathcal{O}_f$: the set of edges $\mathcal{E}_f \subseteq \mathcal{O}_f \times \mathcal{O}_f$, and the weighted adjacency matrix $\mathcal{W}_f = [w_{ij}]_{M\times M}$ with $w_{ij} > 0 \Leftrightarrow (j, i) \in \mathcal{E}_f$ and $w_{ij} = 0$, otherwise. The pinning gain from the leader to the ith follower is represented by w_{i0}, where $w_{i0} > 0$ if information transmission from the leader to the ith follower is feasible; otherwise, $w_{i0} = 0$. A spanning tree is a directed graph in which at least one root node has a directed path to all other nodes.

B. Problem Statement

Consider a HMAS consisting of M followers and one leader. The model of the ith ($i \in \mathcal{O}_f$) follower is given as:

$$\begin{aligned} \dot{x}_i(t) &= A_i x_i(t) + B_i u_i(t) \\ y_i(t) &= C_i x_i(t) \end{aligned} \tag{1}$$

where $x_i \in \mathbb{R}^{n_i}$, $u_i \in \mathbb{R}^{m_i}$, $y_i \in \mathbb{R}^p$ represent the state, control input, and output of the ith follower, respectively, and A_i, B_i, and C_i are the system matrices satisfying $\mathrm{rank}(B_i) = m_i$.

The dynamic of the leader indexed by 0 is described by

$$\begin{aligned} \dot{x}_0(t) &= A_0 x_0(t) + B_0 u_0(t) \\ y_0(t) &= C_0 x_0(t) \end{aligned} \tag{2}$$

where $x_0 \in \mathbb{R}^{n_0}$, $u_0 \in \mathbb{R}^{m_0}$, and $y_0 \in \mathbb{R}^p$ represent the state, command input, and output of the leader, respectively, and A_0, B_0, and C_0 are the system matrices of the leader known to all followers.

Remark 1: The command input $u_0(t)$ is utilized to generate more general reference trajectories. For instance, if the leader, a quadrotor, is modeled with linear dynamics, as discussed in [42], a polynomial reference trajectory can be generated by solving a quadratic program.

This article considers the problem of fixed-time TVF tracking for the HMAS described by (1) and (2). For each follower i, $i \in \mathcal{O}_f$, the piecewise continuous differentiable TVF vector $h_{yi}(t) \in \mathbb{R}^p$ is generated through the system given by

$$\begin{aligned} \dot{h}_{xi}(t) &= A_h h_{xi}(t) \\ h_{yi}(t) &= C_h h_{xi}(t) \end{aligned} \tag{3}$$

Authorized licensed use limited to: Hong Kong Polytechnic University. Downloaded on September 15,2025 at 15:32:38 UTC from IEEE Xplore. Restrictions apply.

where $h_{xi} \in \mathbb{R}^l$, and A_h and C_h are matrices with compatible dimensions.

Remark 2: Equation (3) can be used to generate various formation shapes. Specifically, by setting $A_h = \mathbf{0}_{l\times l}$ and $C_h = \mathrm{I}_{p\times l}$, (3) can specify the nonrotating time-invariant formation shape. In addition, when considering a HMAS moving in the 3-D space, a rotating circular formation, as discussed in [21], [22], [23], and [24], can be generated by setting $A_h = \begin{pmatrix} 0 & 1 \\ -\omega^2 & 0 \end{pmatrix}$ and $C_h = \begin{pmatrix} 1 & 0 \end{pmatrix}$ along each of the X-, Y-, and Z-axes, respectively, where ω represents a positive constant.

This article aims to address the problem as formulated below.

Definition 1 (Fixed-time TVF tracking problem): Given the HMAS consisting of (1) and (2), develop a distributed protocol for each follower so that

$$\lim_{t\to T_f} (y_i(t) - h_{yi}(t) - y_0(t)) = 0 \quad \forall i \in \mathcal{O}_f \tag{4}$$

where $T_f > 0$ represents the convergence time that is independent of the initial conditions.

Remark 3: According to Definition 1, the outputs of the followers are required to achieve the TVF and also to track the reference trajectory generated by the nonautonomous leader in a fixed time. The TVF vector $h_{yi}, i \in \mathcal{O}_f$, represents the desired relative offset of the output y_i from the reference output y_0. It should be noted that the dimension of control does not need to be greater than or equal to that of output for solving the TVF tracking problem (see, for example, [21], [22], [23], [24], and [31]).

III. Main Results

This section presents the main results of this article. To proceed, the following assumptions are put forward.

Assumption 1: The communication topology among the HMAS contains a spanning tree with the leader as its root node.

It follows from Assumption 1 that the corresponding Laplacian matrix can be partitioned as follows:

$$\mathcal{L} = \begin{bmatrix} \mathcal{L}_F & \mathcal{L}_{FL} \\ 0_{1\times M} & 0_{1\times 1} \end{bmatrix}$$

where $\mathcal{L}_{FL} = [-w_{0i}]_{M\times 1}$, $\mathcal{L}_F = [l_{ij}]_{M\times M}$ with $l_{ij} = -w_{ij}$ for $i \neq j$, and $l_{ij} = \sum_{m=1}^{M} w_{im} + w_{i0}$ for $i = j$.

We summarize some important properties of $\mathcal{L}_F$ as follows.

Lemma 1 (See [13]): Under Assumption 1, all eigenvalues of $\mathcal{L}_F$ have positive real parts.

Lemma 2 (See [43]): Under Assumption 1, there exists a real diagonal matrix $\hat{\mathcal{D}}$, ensuring that $\hat{\mathcal{D}}\mathcal{L}_F + \mathcal{L}_F^\top \hat{\mathcal{D}}$ is positive definite.

Let $\lambda_{\min} > 0$ be the smallest eigenvalue of $\hat{\mathcal{D}}\mathcal{L}_F + \mathcal{L}_F^\top\hat{\mathcal{D}}$ and $\mathcal{D} = \mathrm{diag}\{d_1, \ldots, d_M\} := \frac{2\hat{\mathcal{D}}}{\lambda_{\min}}$, where $d_i > 0$, $i = 1, \ldots, M$. Then, via Lemma 2, one has $\mathcal{D}\mathcal{L}_F + \mathcal{L}_F^\top\mathcal{D} \geq 2\mathrm{I}_M$.

In addition, the following standard assumptions are also made.

Assumption 2: For any $i \in \mathcal{O}_f$, (A_i, B_i) are controllable.

Assumption 3: $\|u_0(t)\|_\infty \leq \gamma$, where γ is a positive constant.

Assumption 4: The following regulator equations:

$$\begin{aligned} X_i A_0 &= A_i X_i + B_i U_i \\ 0 &= C_i X_i - C_0 \end{aligned} \tag{5}$$

have solution pairs (X_i, U_i) for all $i \in \mathcal{O}_f$.

Assumption 5: The following regulator equations:

$$\begin{aligned} X_{hi} A_h &= A_i X_{hi} + B_i U_{hi} \\ 0 &= C_i X_{hi} - C_h \end{aligned} \tag{6}$$

have solution pairs (X_{hi}, U_{hi}) for all $i \in \mathcal{O}_f$.

Assumption 6: The linear matrix equation

$$B_i R_i - X_i B_0 = 0 \tag{7}$$

has solution R_i for all $i \in \mathcal{O}_f$.

Remark 4: Assumptions 4–6 are *necessary* for achieving the TVF tracking as in [21], [22], [23], [24], [31], [39], [40], and [41]. As detailed in [44], the regulator equations (5) can be solved if rank $\begin{bmatrix} A_i - \lambda I_{n_i} & B_i \\ C_i & 0 \end{bmatrix} = n_i + p$ holds for all $\lambda \in \sigma(A_0)$, where $\sigma(A_0)$ represents the spectrum of A_0. Assumption 6 is necessary for dealing with the command input of the nonautonomous leader as in [22], [23], [24], and [31]. Moreover, (5) and (7) are satisfied simultaneously for many practical systems. For example, consider a HMAS consisting of several UGVs as followers and a quadrotor as the nonautonomous leader. Utilizing feedback and small perturbation linearization techniques, the followers and the leader can be modeled as first-order integrator systems [18] and second-order linear dynamics [45], respectively. Given that the HMAS moves in the XY plane, it can be verified that with $X_i = \mathrm{I}_2 \otimes \begin{pmatrix} 1 & 0 \end{pmatrix}$, $U_i = \mathrm{I}_2 \otimes \begin{pmatrix} 0 & 1 \end{pmatrix}$, and $R_i = \mathbf{0}_{2\times 2}$, the regulator equations (5) and (7) can be satisfied simultaneously.

We present distributed fixed-time observers and fixed-time TVF tracking protocols for the HMAS with the nonautonomous leader subsequently.

A. Distributed Fixed-Time Observers for Nonautonomous Leader

Given that not all followers have access to the state of the leader, it is crucial to develop distributed observers to estimate the state of the leader within a fixed time in this work.

The distributed observer is constructed for each follower as follows:

$$\begin{aligned} \dot{\eta}_i = {} & A_0\eta_i - c_1\varepsilon_i - c_2\mathrm{sig}^\alpha(\varepsilon_i) - c_3\mathrm{sig}^\beta(\varepsilon_i) \\ & - \rho B_0 \mathrm{sign}(B_0^\top \bar{\varepsilon}_i) \end{aligned} \tag{8a}$$

$$\varepsilon_i = \sum_{j=1}^{M} w_{ij}(\eta_i - \eta_j) + w_{i0}(\eta_i - x_0) \tag{8b}$$

$$\bar{\varepsilon}_i = c_1\varepsilon_i + c_2\mathrm{sig}^\alpha(\varepsilon_i) + c_3\mathrm{sig}^\beta(\varepsilon_i) \tag{8c}$$

where η_i represents the state of the distributed observer used to estimate x_0, ε_i denotes the neighboring relative estimation error, and the parameters c_1, c_2, c_3, α, β, and ρ are positive constants that will be decided later.

Authorized licensed use limited to: Hong Kong Polytechnic University. Downloaded on September 15,2025 at 15:32:38 UTC from IEEE Xplore. Restrictions apply.

The following theorem shows the effectiveness of the proposed distributed fixed-time observers.

Theorem 1: Consider the distributed observers (8a)–(8c). Let c_1, c_2, c_3, α, β, and ρ be chosen such that $c_1 > \|\mathcal{D}\otimes A_0\|$, $c_2>0, c_3>0, 0<\alpha<1, \beta>\frac{1}{\alpha}>1$, and $\rho\geq\gamma$. There exists a settling time $T_\eta \geq 0$ regardless of any initial states, such that

$$\lim_{t\to T_\eta}(\eta_i(t)-x_0(t))=0$$
$$\eta_i(t)-x_0(t)=0,\ t\geq T_\eta \quad \forall i\in\mathcal{O}_f. \tag{9}$$

Proof: Letting $\eta=[\eta_1^\top,\ldots,\eta_M^\top]^\top$, $\varepsilon=[\varepsilon_1^\top,\ldots,\varepsilon_M^\top]^\top$, and $\bar{\varepsilon}=[\bar{\varepsilon}_1^\top,\ldots,\bar{\varepsilon}_M^\top]^\top$, one can obtain from (8) that

$$\dot{\eta}=(\mathrm{I}_M\otimes A_0)\eta-(\mathrm{I}_M\otimes \mathrm{I}_{n_0})\bar{\varepsilon}-\rho(\mathrm{I}_M\otimes B_0)f \tag{10}$$

where $f=[f_1^\top,\ldots,f_2^\top]^\top$ with $f_i=\mathrm{sign}(B_0^\top\bar{\varepsilon}_i(t))$.

Let $\tilde{\eta}_i=\eta_i-x_0$. From (2) and (8), one has

$$\dot{\tilde{\eta}}_i=A_0\tilde{\eta}_i-c_1\varepsilon_i-c_2\mathrm{sig}^\alpha(\varepsilon_i)-c_3\mathrm{sig}^\beta(\varepsilon_i)-\rho B_0 f_i-B_0u_0. \tag{11}$$

Let $\tilde{\eta}=[\tilde{\eta}_1^\top,\ldots,\tilde{\eta}_M^\top]^\top$. Then, system (11) can be rewritten in the following compact form:

$$\dot{\tilde{\eta}}=(\mathrm{I}_M\otimes A_0)\tilde{\eta}-\rho(\mathrm{I}_M\otimes B_0)f-(\mathrm{I}_M\otimes B_0)\bar{u}_0-(\mathrm{I}_M\otimes \mathrm{I}_{n_0})\bar{\varepsilon} \tag{12}$$

where $\bar{u}_0=1_M\otimes u_0(t)$.

Noting that $\varepsilon=(\mathcal{L}_F\otimes \mathrm{I}_{n_0})\tilde{\eta}$, it then follows from (12) that:

$$\dot{\varepsilon}=(I_M\otimes A_0)\varepsilon-(\mathcal{L}_F\otimes \mathrm{I}_{n_0})\bar{\varepsilon}-\rho(\mathcal{L}_F\otimes B_0)f-(\mathcal{L}_F\otimes B_0)\bar{u}_0 \tag{13}$$

where $\bar{u}_0=1_M\otimes u_0(t)$ and $f=[f_1^\top,\ldots,f_2^\top]^\top$ with $f_i=\mathrm{sign}(B_0^\top\bar{\varepsilon}_i(t))$.

Take into account the following Lyapunov function candidate:

$$V_1=\sum_{i=1}^M\left(\frac{c_2d_i}{1+\alpha}\|\varepsilon_i\|_{1+\alpha}^{1+\alpha}+\frac{c_3d_i}{1+\beta}\|\varepsilon_i\|_{1+\beta}^{1+\beta}\right)+\frac{c_1}{2}\varepsilon^\top(\mathcal{D}\otimes I_{n_0})\varepsilon. \tag{14}$$

The time derivative of (14) along with the trajectories of (13) satisfies

$$\begin{aligned}\dot{V}_1=&\sum_{i=1}^M\left(c_2d_i\mathrm{sig}^\alpha(\varepsilon_i)+c_3d_i\mathrm{sig}^\beta(\varepsilon_i)\right)^\top\dot{\varepsilon}_i\\&+c_1\varepsilon^\top(\mathcal{D}\otimes I_{n_0})\dot{\varepsilon}\\=&\bar{\varepsilon}^\top(\mathcal{D}\otimes A_0)\varepsilon-\frac{1}{2}\bar{\varepsilon}^\top\left((\mathcal{L}_F^\top\mathcal{D}+\mathcal{D}\mathcal{L}_F)\otimes I_{n_0}\right)\bar{\varepsilon}\\&-\rho\bar{\varepsilon}^\top(\mathcal{D}\mathcal{L}_F\otimes B_0)f-\bar{\varepsilon}^\top(\mathcal{D}\mathcal{L}_F\otimes B_0)\bar{u}_0(t).\end{aligned} \tag{15}$$

Noting that $\mathcal{D}\mathcal{L}_F+\mathcal{L}_F^\top\mathcal{D}\geq 2\mathrm{I}_M$, via Young's inequality, one has

$$\bar{\varepsilon}^\top(\mathcal{D}\otimes A_0)\varepsilon-\frac{1}{2}\bar{\varepsilon}^\top\left((\mathcal{L}_F^\top\mathcal{D}+\mathcal{D}\mathcal{L}_F)\otimes I_{n_0}\right)\bar{\varepsilon}\leq\frac{1}{2}(\|\mathcal{D}\otimes A_0\|^2\|\varepsilon\|^2-\|\bar{\varepsilon}\|^2). \tag{16}$$

Since $f_i=\mathrm{sign}(B_0^\top\bar{\varepsilon}_i(t))$, one has $\bar{\varepsilon}_i^\top B_0f_i=\|B_0^\top\bar{\varepsilon}_i\|_1$ and $\bar{\varepsilon}_i^\top B_0f_j\leq\|B_0^\top\bar{\varepsilon}_i\|_1$. Then, one can derive that

$$\begin{aligned}&-\rho\bar{\varepsilon}^\top(\mathcal{D}\mathcal{L}_F\otimes B_0)f\\&=-\rho\sum_{i=1}^M d_i\bar{\varepsilon}_i^\top B_0\left(\sum_{j=1}^M w_{ij}(f_i-f_j)+w_{i0}f_i\right)\\&\leq-\rho\sum_{i=1}^M d_iw_{i0}\left\|B_0^T\bar{\varepsilon}_i\right\|_1.\end{aligned} \tag{17}$$

From Assumption 3, one has

$$\begin{aligned}-\bar{\varepsilon}^\top(\mathcal{D}\mathcal{L}_F\otimes B_0)\bar{u}_0&=-\sum_{i=1}^M d_iw_{i0}\bar{\varepsilon}_i^\top B_0u_0\\&\leq\gamma\sum_{i=1}^M d_iw_{i0}\left\|B_0^\top\bar{\varepsilon}_i\right\|_1.\end{aligned} \tag{18}$$

Note that $\rho\geq\gamma$. From (16) to (18), one can obtain that

$$\dot{V}_1\leq\frac{1}{2}(\|\mathcal{D}\otimes A_0\|^2\|\varepsilon\|^2-\|\bar{\varepsilon}\|^2). \tag{19}$$

Note that $\|\bar{\varepsilon}\|^2=\sum_{i=1}^M\|\bar{\varepsilon}_i\|^2$, where $\bar{\varepsilon}_i=c_1\varepsilon_i+c_2\mathrm{sig}^\alpha(\varepsilon_i)+c_3\mathrm{sig}^\beta(\varepsilon_i)$. Since $c_i>0$, $i=1,2,3$, the terms $c_1\varepsilon_i$, $c_2\mathrm{sig}^\alpha(\varepsilon_i)$, and $c_3\mathrm{sig}^\beta(\varepsilon_i)$ have componentwise sign consistency across all their respective elements. Then, from (8b), one has

$$\begin{aligned}\|\bar{\varepsilon}\|^2=&\sum_{i=1}^M\|c_1\varepsilon_i+c_2\mathrm{sig}^\alpha(\varepsilon_i)+c_3\mathrm{sig}^\beta(\varepsilon_i)\|^2\\=&\sum_{i=1}^M\Big(c_1^2\|\varepsilon_i\|^2+c_2^2\|\varepsilon_i\|_{2\alpha}^{2\alpha}+c_3^2\|\varepsilon_i\|_{2\beta}^{2\beta}\\&+2c_1c_2\|\varepsilon_i\|_{1+\alpha}^{1+\alpha}+2c_1c_3\|\varepsilon_i\|_{1+\beta}^{1+\beta}+2c_2c_3\|\varepsilon_i\|_{\alpha+\beta}^{\alpha+\beta}\Big)\\\geq&\sum_{i=1}^M c_1^2\|\varepsilon_i\|^2+\sum_{i=1}^M c_2^2\|\varepsilon_i\|_{2\alpha}^{2\alpha}\\&+\sum_{i=1}^M c_3^2\|\varepsilon_i\|_{2\beta}^{2\beta}.\end{aligned} \tag{20}$$

Noting that $0<\alpha<1$ and $\beta>1$, by Lemma 3 given in Appendix, one has

$$\sum_{i=1}^M\|\varepsilon_i\|_{2\alpha}^{2\alpha}\geq\left(\|\varepsilon\|^2\right)^\alpha, \tag{21}$$

$$\sum_{i=1}^M\|\varepsilon_i\|_{2\beta}^{2\beta}\geq\frac{1}{(n_0M)^{\beta-1}}\left(\|\varepsilon\|^2\right)^\beta. \tag{22}$$

From (20) to (22), one has

$$\|\bar{\varepsilon}\|^2\geq c_1^2\|\varepsilon\|^2+c_2^2\left(\|\varepsilon\|^2\right)^\alpha+\frac{c_3^2}{(n_0M)^{\beta-1}}\left(\|\varepsilon\|^2\right)^\beta. \tag{23}$$

Substituting (23) into (19), one has

$$\begin{aligned}\dot{V}_1\leq&-\frac{1}{2}(c_1^2-\|\mathcal{D}\otimes A_0\|^2)\|\varepsilon\|^2-\frac{c_2^2}{2}\left(\|\varepsilon\|^2\right)^\alpha\\&-\frac{c_3^2}{2(n_0M)^{\beta-1}}\left(\|\varepsilon\|^2\right)^\beta\\\leq&-k_e\left(\|\varepsilon\|^2+\left(\|\varepsilon\|^2\right)^\alpha+\left(\|\varepsilon\|^2\right)^\beta\right)\end{aligned} \tag{24}$$

where $k_e=\min\{\frac{1}{2}(c_1^2-\|\mathcal{D}\otimes A_0\|^2),\frac{c_2^2}{2},\frac{c_3^2}{2(n_0M)^{\beta-1}}\}>0$.

Authorized licensed use limited to: Hong Kong Polytechnic University. Downloaded on September 15,2025 at 15:32:38 UTC from IEEE Xplore. Restrictions apply.

Since $0<\alpha<1$ and $\beta>1$, via Lemma 3, one has

$$\sum_{i=1}^{M}\frac{c_2 d_i}{1+\alpha}\|\varepsilon_i\|_{1+\alpha}^{1+\alpha}\le \bar{c}_2(\|\varepsilon\|^2)^{\frac{1+\alpha}{2}} \tag{25}$$

$$\sum_{i=1}^{M}\frac{c_3 d_i}{1+\beta}\|\varepsilon_i\|_{1+\beta}^{1+\beta}\le \bar{c}_3(\|\varepsilon\|^2)^{\frac{1+\beta}{2}} \tag{26}$$

where $\bar{c}_2=(\frac{c_2 d_{\max}}{1+\alpha})(n_0 M)^{\frac{1-\alpha}{2}}$, $\bar{c}_3=\frac{c_3 d_{\max}}{1+\beta}$, and $d_{\max}=\max\{d_1,\ldots,d_M\}$.

Note that $0<\frac{2\alpha}{1+\alpha}<1$. It then follows from (25), (26), and Lemma 3 that:

$$V_1^{\frac{2\alpha}{1+\alpha}}\le k_\alpha\left((\|\varepsilon\|^2)^{\frac{2\alpha}{1+\alpha}}+(\|\varepsilon\|^2)^{\alpha}+(\|\varepsilon\|^2)^{\frac{\alpha(1+\beta)}{1+\alpha}}\right) \tag{27}$$

where $k_\alpha=\max\{(\frac{c_1 d_{\max}}{2})^{\frac{2\alpha}{1+\alpha}},\bar{c}_2^{\frac{2\alpha}{1+\alpha}},\bar{c}_3^{\frac{2\alpha}{1+\alpha}}\}$.

Since $\alpha<\frac{2\alpha}{1+\alpha}<1$ and $\alpha<\frac{\alpha(1+\beta)}{1+\alpha}<\beta$, one has

$$(\|\varepsilon\|^2)^{\frac{2\alpha}{1+\alpha}}\le\|\varepsilon\|^2+(\|\varepsilon\|^2)^{\alpha} \tag{28}$$

$$(\|\varepsilon\|^2)^{\frac{\alpha(1+\beta)}{1+\alpha}}\le(\|\varepsilon\|^2)^{\alpha}+(\|\varepsilon\|^2)^{\beta}. \tag{29}$$

It follows from (28) and (29) that:

$$V_1^{\frac{2\alpha}{1+\alpha}}\le k_\alpha\left(\|\varepsilon\|^2+3(\|\varepsilon\|^2)^{\alpha}+(\|\varepsilon\|^2)^{\beta}\right). \tag{30}$$

Similarly, since $\frac{2\beta}{1+\beta}>1$, via Lemma 3, one can obtain from (25) and (26) that

$$V_1^{\frac{2\beta}{1+\beta}}\le k_\beta\left((\|\varepsilon\|^2)^{\frac{2\beta}{1+\beta}}+(\|\varepsilon\|^2)^{\frac{\beta(1+\alpha)}{1+\beta}}+(\|\varepsilon\|^2)^{\beta}\right) \tag{31}$$

where $k_\beta=\max\{(\frac{c_1 d_{\max}}{2})^{\frac{2\beta}{1+\beta}},\bar{c}_2^{\frac{2\beta}{1+\beta}},\bar{c}_3^{\frac{2\beta}{1+\beta}}\}\times 3^{\frac{\beta-1}{\beta+1}}$.

Noting that $1<\frac{2\beta}{1+\beta}<\beta$ and $\alpha<\frac{\beta(1+\alpha)}{1+\beta}<\beta$, one has

$$(\|\varepsilon\|^2)^{\frac{2\beta}{1+\beta}}\le\|\varepsilon\|^2+(\|\varepsilon\|^2)^{\beta} \tag{32}$$

$$(\|\varepsilon\|^2)^{\frac{\beta(1+\alpha)}{1+\beta}}\le(\|\varepsilon\|^2)^{\alpha}+(\|\varepsilon\|^2)^{\beta}. \tag{33}$$

From (32) and (33), one can derive that

$$V_1^{\frac{2\beta}{1+\beta}}\le k_\beta\left(\|\varepsilon\|^2+3(\|\varepsilon\|^2)^{\beta}+(\|\varepsilon\|^2)^{\alpha}\right). \tag{34}$$

Combining (30) and (34), one has

$$\begin{aligned}&\frac{1}{4k_\alpha}V_1^{\frac{2\alpha}{1+\alpha}}+\frac{1}{4k_\beta}V_1^{\frac{2\beta}{1+\beta}}\\&\le\left(\|\varepsilon\|^2+(\|\varepsilon\|^2)^{\beta}+(\|\varepsilon\|^2)^{\alpha}\right).\end{aligned} \tag{35}$$

Substituting (35) into (24), one has

$$\dot{V}_1\le-\frac{k_e}{4k_\alpha}V_1^{\frac{2\alpha}{1+\alpha}}-\frac{k_e}{4k_\beta}V_1^{\frac{2\beta}{1+\beta}}. \tag{36}$$

By Lemma 4 in the Appendix, one can get that system (13) is fixed-time stable. The corresponding fixed settling time $T_\eta\le\frac{4k_\alpha(1+\alpha)}{k_e(1-\alpha)}+\frac{4k_\beta(1+\beta)}{k_e(\beta-1)}$. Moreover, since $\varepsilon(t)=(\mathcal{L}_F\otimes \mathrm{I}_{n_0})\tilde{\eta}(t)$ and $\mathcal{L}_F$ is nonsingular, we have $\lim_{t\to T_\eta}(\eta_i(t)-x_0(t))=0$ and $\eta_i(t)-x_0(t)=0$ for $t\ge T_\eta$. Thus, the proof is completed.

B. Fixed-Time TVF Tracking Protocols

With the distributed fixed-time observer described in (8a)–(8c), we proceed to introduce fixed-time TVF tracking protocols in this part.

For each follower, the following observer-based fixed-time TVF tracking protocol is proposed:

$$u_i(t)=U_i\eta_i(t)+U_{hi}h_{xi}(t)+v_i(t),\ i\in\mathcal{O}_f \tag{37}$$

where U_i and U_{hi} are the solutions to (5) and (6), respectively, and $v_i(t)$ will be determined later for achieving fixed-time tracking.

Since only the followers in direct communication with the leader can access to $x_0(t)$, the fixed-time tracking control component $v_i(t)$ for other followers should also be designed based on the estimated state from the distributed observer (8). Define $\hat{e}_i=x_i-X_i\eta_i-X_{hi}h_{xi}$. Under Assumptions 4–6, one can obtain from (1), (8), and (37) that

$$\dot{\hat{e}}_i=A_i\hat{e}_i+B_i v_i-X_i\tilde{\varepsilon}_i \tag{38}$$

where $\tilde{\varepsilon}_i=-c_1\varepsilon_i-c_2\mathrm{sig}^{\alpha}(\varepsilon_i)-c_3\mathrm{sig}^{\beta}(\varepsilon_i)-\rho B_0\mathrm{sign}(B_0^{\top}\bar{\varepsilon}_i)$, and ε_i and $\bar{\varepsilon}_i$ are defined in (8b) and (8c), respectively.

Since (A_i,B_i) is controllable and $\mathrm{rank}(B_i)=m_i$, via Lemma 5 given in the Appendix, there exists a linear coordinate transformation $\hat{\xi}_i=T_i\hat{e}_i=[\hat{\xi}_{i1,1},\ldots,\hat{\xi}_{i1,\rho_1},\ldots,\hat{\xi}_{im_i,1},\ldots,\hat{\xi}_{im_i,\rho_{m_i}}]^{\top}$, where $\rho_j, j=1,\ldots,m_i$, denotes the controllability index of $\hat{\xi}_{ij}$. Letting $\hat{\xi}_i^{\rho}=[\hat{\xi}_{i1,\rho_1},\ldots,\hat{\xi}_{im_i,\rho_{m_i}}]^{\top}$, the integral sliding surface s_i is constructed as follows:

$$s_i=\hat{\xi}_i^{\rho}-\omega_{i,\mathrm{int}} \tag{39}$$

where

$$\begin{aligned}\dot{\omega}_{i,\mathrm{int}}&=\omega_i\\ \omega_i&=[\omega_{i1},\ldots,\omega_{ij},\ldots,\omega_{im_i}]^{\top}\\ \omega_{ij}&=-\sum_{h=1}^{\rho_j}\left(k_{ij,h}\mathrm{sig}^{p_{ij,h}}(\hat{\xi}_{ij,h})+\bar{k}_{ij,h}\mathrm{sig}^{q_{ij,h}}(\hat{\xi}_{ij,h})\right)\end{aligned}$$

$k_{ij,h}$, $\bar{k}_{ij,h}$, $p_{ij,h}$, $q_{ij,h}$, $j=1,\ldots,m_i$, $h=1,\ldots,\rho_j$, are the positive gains that can be designed as in Lemma 6 in the Appendix.

Then, $v_i(t)$ is designed as follows:

$$v_i=M_i^{-1}(\Omega_i-G_i\hat{e}_i) \tag{40}$$

where

$$\Omega_i=\omega_i-\bar{\gamma}_i\mathrm{sign}(s_i)-k_\mu\left(\mathrm{sig}^{\mu}(s_i)+\mathrm{sig}^{\frac{1}{\mu}}(s_i)\right)$$

G_i and M_i are given as in Lemma 5, the real numbers $\bar{\gamma}_i$, μ, and k_μ are chosen such that $\bar{\gamma}_i\ge\gamma\|M_iR_i\|_\infty$, $\mu>1$, and $k_\mu>1\min\{m_i^{\frac{1-\mu}{2}},1\}>0$.

Remark 5: Under Assumption 2 and $\mathrm{rank}(B_i)=m_i$, via Lemma 5, there exists a nonsingular matrix M_i for each follower to obtain the fixed-time tracking control component $v_i(t)$.

We are ready to present the main result of this section.

Theorem 2: Consider the HMAS consisting of (1) and (2) under Assumptions 1–6. The fixed-time TVF tracking problem described by (4) is solved under the protocol defined in (37) and (40).

Proof: The proof of Theorem 2 includes three steps. First, we show that the TVF tracking errors are bounded in $[0,T_\eta)$, i.e., no finite-time escape occurs. Second, we prove that the sliding mode will be reached in a fixed time. Lastly, we show that when

Authorized licensed use limited to: Hong Kong Polytechnic University. Downloaded on September 15,2025 at 15:32:38 UTC from IEEE Xplore. Restrictions apply.

$s_i(t)=0$, the TVF tracking errors converge to zero in a fixed time.

Step 1: Let $\Delta_i=T_iX_i\tilde{\varepsilon}_i=[\Delta_{i1,1},\ldots,\Delta_{i1,\rho_1},\ldots,\Delta_{im_i,1},\ldots,\Delta_{im_i,\rho_{m_i}}]^\top$ and $\Delta_i^\rho=[\Delta_{i1,\rho_1},\ \ldots,\Delta_{im_i,\rho_{m_i}}]^\top$. Via Lemma 5, from (38) and (40), one has

$$\begin{aligned}\dot{\hat{\xi}}_i^\rho&=G_i\hat{e}_i+M_iv_i-\Delta_i^\rho\\&=\omega_i-\bar{\gamma}_i\text{sign}(s_i)-k_\mu(\text{sig}^\mu(s_i)+\text{sig}^{\frac{1}{\mu}}(s_i))-\Delta_i^\rho.\end{aligned}\tag{41}$$

From (41), the time derivative of s_i can be derived as

$$\dot{s}_i=-\bar{\gamma}_i\text{sign}(s_i)-k_\mu(\text{sig}^\mu(s_i)+\text{sig}^{\frac{1}{\mu}}(s_i))-\Delta_i^\rho.\tag{42}$$

Consider the Lyapunov function candidate $V_2=\frac{1}{2}s_i^\top s_i$. Taking the time derivative of V_2 along with the trajectories of system (42) yields

$$\dot{V}_2=-\bar{\gamma}_i\|s_i\|_1-s_i\Delta_i^\rho-k_\mu\left(\|s_i\|_{\mu+1}^{\mu+1}+\|s_i\|_{\frac{1}{\mu}+1}^{\frac{1}{\mu}+1}\right).\tag{43}$$

Via Young's inequality, one can get

$$-s_i\Delta_i^\rho\le\|s_i\|^2+\frac{1}{4}\|\Delta_i^\rho\|^2.\tag{44}$$

Noting that $\mu>1$ and $\frac{1}{2}<\frac{1+\mu}{2\mu}<1$, via Lemma 3, one can obtain that

$$\|s_i\|_{\mu+1}^{\mu+1}\ge m_i^{\frac{1-\mu}{2}}(\|s_i\|^2)^{\frac{\mu+1}{2}}\tag{45}$$

$$\|s_i\|_{\frac{1}{\mu}+1}^{\frac{1}{\mu}+1}\ge(\|s_i\|^2)^{\frac{1+\mu}{2\mu}}.\tag{46}$$

Since $\frac{1+\mu}{2\mu}<1<\frac{\mu+1}{\mu}$, one has

$$\|s_i\|^2\le(\|s_i\|^2)^{\frac{1+\mu}{2\mu}}+(\|s_i\|^2)^{\frac{\mu+1}{\mu}}.\tag{47}$$

It follows from (45) to (47) that:

$$-k_\mu\left(\|s_i\|_{\mu+1}^{\mu+1}+\|s_i\|_{\frac{1}{\mu}+1}^{\frac{1}{\mu}+1}\right)\le-\bar{k}_\mu\|s_i\|^2\tag{48}$$

where $\bar{k}_\mu=\min\{m_i^{\frac{1-\mu}{2}},1\}k_\mu$.

Note that $-\bar{\gamma}_i\|s_i\|_1\le0$. It follows from (44) and (48) that:

$$\dot{V}_2\le-\epsilon V_2+\frac{l}{4}\|\Delta_i^\rho\|^2\tag{49}$$

where $\epsilon=2(\bar{k}_\mu-1)>0$.

Recalling Theorem 1, which shows that the distributed fixed-time observer error system (13) is fixed-time stable, one has that $\tilde{\varepsilon}_i$, Δ_i, and Δ_i^ρ are all bounded in $[0,T_\eta)$. Therefore, there is a constant $\mathcal{C}$ such that

$$\dot{V}_2\le-\epsilon V_2+\mathcal{C}\tag{50}$$

holds for $t\in[0,T_\eta)$.

From (50), one can obtain that V_2 is bounded in $[0,T_\eta)$, which, in turn, implies that s_i is bounded in $[0,T_\eta)$. Noting that $s_i=\hat{\xi}_i^\rho-\omega_{i,\text{int}}=[s_{i1},\ldots,s_{im_i}]^\top$ with $s_{ij}=\hat{\xi}_{ij,\rho_j}+\sum_{k=1}^{\rho_j}k_{ij,k}\int_0^t\text{sig}^{p_{ij,k}}(\hat{\xi}_{ij,k}(\tau))d\tau+\sum_{k=1}^{\rho_j}\bar{k}_{ij,k}\int_0^t\text{sig}^{q_{ij,k}}(\hat{\xi}_{ij,k}(\tau))d\tau$ and the boundedness of Δ_i, one can derive that $\hat{\xi}_i$ is bounded in $[0,T_\eta)$. Since $\hat{\xi}_i=T_i\hat{e}_i$ and T_i is invertible, we can conclude that $\hat{e}_i$ is also bounded in $[0,T_\eta)$, i.e., no finite-time escape occurs.

Step 2: Via Theorem 1, one has that $\eta_i(t)=x_0(t)$ holds for $t\ge T_\eta$, which implies that $\hat{e}_i=e_i=x_i-X_ix_0-X_{hi}h_{xi}$. It follows from (1), (2), and (37) that:

$$\dot{e}_i=A_ie_i+B_i(v_i-R_iu_0).\tag{51}$$

Via Lemma 5, one can obtain from (40) and (51) that

$$\begin{aligned}\dot{\xi}_i^\rho&=G_ie_i+M_i(v_i-R_iu_0)\\&=\omega_i-\bar{\gamma}_i\text{sign}(s_i)-k_\mu(\text{sig}^\mu(s_i)+\text{sig}^{\frac{1}{\mu}}(s_i))\\&\quad-M_iR_iu_0.\end{aligned}\tag{52}$$

Taking the time derivative of s_i yields

$$\begin{aligned}\dot{s}_i=&-\bar{\gamma}_i\text{sign}(s_i)-k_\mu(\text{sig}^\mu(s_i)+\text{sig}^{\frac{1}{\mu}}(s_i))\\&-M_iR_iu_0.\end{aligned}\tag{53}$$

Consider the Lyapunov function candidate $V_3=\frac{1}{2}s_i^\top s_i$. Its time derivative along with the trajectories of system (53) can be obtained as

$$\begin{aligned}\dot{V}_3=&-\bar{\gamma}_i\|s_i\|_1-s_i^\top M_iR_iu_0\\&-k_\mu(\|s_i\|_{\mu+1}^{\mu+1}+\|s_i\|_{\frac{1}{\mu}+1}^{\frac{1}{\mu}+1}).\end{aligned}\tag{54}$$

Noting that $\bar{\gamma}_i\ge\gamma\|M_iR_i\|_\infty$, from Assumption 3, one has

$$\begin{aligned}&-\bar{\gamma}_i\|s_i\|_1-s_i^\top M_iR_iu_0\\&\le-(\bar{\gamma}_i-\gamma\|M_iR_i\|_\infty)\|s_i\|_1\le0.\end{aligned}\tag{55}$$

Noting that $\mu>1$ and $\frac{1}{2}<\frac{1+\mu}{2\mu}<1$, via Lemma 3, one has

$$\|s_i\|_{\mu+1}^{\mu+1}\ge m_i^{\frac{1-\mu}{2}}(\|s_i\|^2)^{\frac{\mu+1}{2}}\tag{56}$$

$$\|s_i\|_{\frac{1}{\mu}+1}^{\frac{1}{\mu}+1}\ge(\|s_i\|^2)^{\frac{1+\mu}{2\mu}}.\tag{57}$$

Substituting (55)–(57) into (54), one has

$$\dot{V}_3\le-\bar{k}_{si}V_3^{\frac{\mu+1}{2}}-\hat{k}_sV_3^{\frac{\mu+1}{2\mu}}\tag{58}$$

where $\bar{k}_{si}=m_i^{\frac{1-\mu}{2}}2^{\frac{\mu+1}{2}}$ and $\hat{k}_s=2^{\frac{\mu+1}{2\mu}}$.

Therefore, by Lemma 4, system (53) will reach the sliding surface $s_i=0$ in a fixed time. Moreover, for all $i\in\mathcal{O}_f$, there is a constant T_c regardless of initial states such that $s_i(t)=0$ for $t\ge T_\eta+T_c$, where T_η is given in Theorem 1 and $T_c\le\max\{T_{c1},\ldots,T_{cM}\}$ with $T_{ci}=\frac{2\mu}{k_{si}(\mu-1)}+\frac{2}{\hat{k}_s(\mu-1)}$.

Step 3: When $s_i(t)\equiv0$, one can obtain that $\dot{s}_i(t)=0$. Then, from (53), we have that the equivalent control of $-\bar{\gamma}_i\text{sign}(s_i)-k_\mu(\text{sig}^\mu(s_i)+\text{sig}^{\frac{1}{\mu}}(s_i))$ is equal to $M_iR_iu_0$. Substituting this into (52), via Lemma 5, one can obtain that the dynamics of $\xi_{ij}(t)$, $j=1,\ldots,m_i$, have the following form:

$$\begin{cases}\dot{\xi}_{ij,1}=\xi_{ij,2}\\\dot{\xi}_{ij,2}=\xi_{ij,3}\\\vdots\\\dot{\xi}_{ij,\rho_j}=\sum\limits_{k=1}^{\rho_j}(k_{ij,k}\text{sig}^{p_{ij,k}}(\xi_{ij,k}\\\qquad+\bar{k}_{ij,k}\text{sig}^{q_{ij,k}}(\xi_{ij,k})\end{cases}.\tag{59}$$

Authorized licensed use limited to: Hong Kong Polytechnic University. Downloaded on September 15,2025 at 15:32:38 UTC from IEEE Xplore. Restrictions apply.

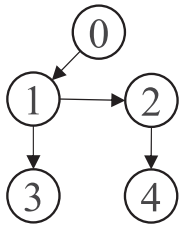

Fig. 1. Communication network.

From Lemma 6, it can be concluded that for all $j \in \{1, \ldots, m_i\}$, system (59) is fixed-time stable, and the settling time can be upper bounded by $T_f \leq T_\eta + T_s + T_\xi$, where T_ξ can be determined based on Lemma 6. Since $\xi_i(t) = T_i e_i(t), T_i$ is invertible, and $e_{yi}(t) = C_i e_i(t) = y_i(t) - h_{yi}(t) - y_0(t)$, we can derive that $\lim_{t \to T_f} e_{yi}(t) = 0$ and $e_{yi}(t) = 0$ for $t \geq T_f$, i.e., the fixed-time TVF tracking problem described by (4) is solved. The theorem is thus proved.

Remark 6: It is noted that the right-hand sides of (8) and (38) are discontinuous at zeros, and the solutions of (8) and (38) are defined in the sense of Filippov [46].

Remark 7: Utilizing the technique of coordinate transformation, the original system (38) can be decomposed into m_i single-input systems in canonical controller form, with coupling occurring through the last line of each block. Then, a fixed-time TVF tracking control protocol is developed using the sliding mode technique. This approach eliminates the need to compute the generalized inverse matrix of the input matrix of the follower, thus removing the requirement for the input matrix of the followers to be of full row rank, as often required in [39], [40], and [41].

Remark 8: In contrast to the recent work on heterogeneous underactuated agents in [16], more general agent dynamics and a nonautonomous leader are considered in this work. Moreover, unlike the studies [16] and [21] with asymptotic convergence, and [32] with finite-time convergence, our fixed-time protocol addresses the challenges posed by complex relationships among fractional powers, asymmetric Laplacian matrix of directed topology, and nonlinear functions compensating for the command input. Consequently, the fixed-time TVF tracking problem described by (4) is solved under our proposed protocol.

IV. Simulation

Consider a group of HMAS consisting of four followers and one leader. The communication network is illustrated in Fig. 1.

Example 1: The system matrices of the followers are borrowed from [47], described as follows:

$$A_i = \begin{pmatrix} 0 & 1 & 0 \\ 0 & d_i & c_i \\ 0 & b_i & a_i \end{pmatrix}, \quad B_i = \begin{pmatrix} 0 & 0 \\ e_i & 0 \\ 0 & f_i \end{pmatrix}$$

$$C_i = \begin{pmatrix} 1 & 0 & 0 \\ 0 & 1 & 0 \end{pmatrix}, \quad i = 1, 2, 3, 4$$

where the parameters $\{a_i, b_i, c_i, d_i, e_i, f_i\}$ are chosen as $\{-4, 0, 1, 1, 1, 1\}, \{-2, -1, 2, 0, 1, 1\}, \{-2, 0, 2, 1, 1, 1\}$, and $\{-3, -1, 1, 0, 1, 1\}$.

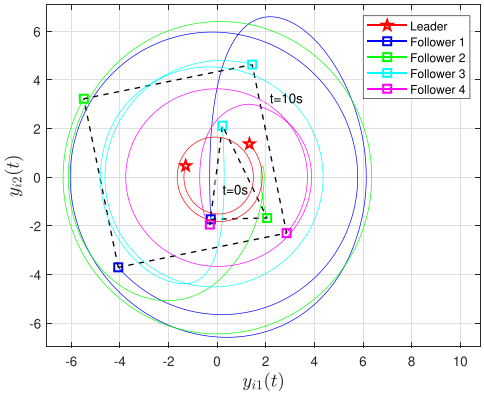

Fig. 2. Output trajectories of the HMAS for Example 1.

The dynamics of the nonautonomous leader (2) are described by

$$A_0 = \begin{pmatrix} 0 & 1 & 0 \\ -1 & 0 & 0 \\ 0 & 0 & 0 \end{pmatrix}, \; B_0 = \begin{pmatrix} 0 & 0 \\ 1 & 0 \\ 0 & 1 \end{pmatrix}, \; C_0 = \begin{pmatrix} 1 & 0 & 0 \\ 0 & 1 & 0 \end{pmatrix}.$$

The command input is given as $u_0(t) = [-0.2\cos(t) \; -0.2\sin(t)]^\top$, and $\|u_0(t)\|_\infty \leq \gamma = 0.2$.

The TVF vector is set as follows:

$$h_{xi} = 5 \begin{pmatrix} \sin\left(t + \frac{(i-1)\pi}{2}\right) \\ \cos\left(t + \frac{(i-1)\pi}{2}\right) \end{pmatrix}, \; i = 1, 2, 3, 4$$

and $h_{yi} = h_{xi}$. Solving (5)–(7) yields

$$X_i = \begin{pmatrix} 1 & 0 & 0 \\ 0 & 1 & 0 \\ -\frac{1}{c_i} & 0 & 0 \end{pmatrix}, \; X_{hi} = \begin{pmatrix} 1 & 0 \\ 0 & 1 \\ b_i & 0 \end{pmatrix}, R_i = \begin{pmatrix} \frac{1}{e_i} & 0 \\ 0 & \frac{1}{f_i} \end{pmatrix}$$

$$U_i = \begin{pmatrix} 0 & -\frac{d_i}{e_i} & -\frac{c_i}{e_i} \\ -\frac{a_i}{c_i f_i} & \frac{-c_i b_i - 1}{c_i f_i} & 0 \end{pmatrix}, U_{hi} = \begin{pmatrix} \frac{-b_i c_i - 1}{e_i} & -\frac{d_i}{e_i} \\ -\frac{a_i b_i}{f_i} & 0 \end{pmatrix}.$$

The parameters in the distributed fixed-time observer (8) and controller (40) are given as $c_1 = 7$, $c_2 = 5$, $c_3 = 6$, $\alpha = 7/9$, $\beta = 907/700$, $\rho = 0.3$, $\bar{\gamma}_i = 1.2$, $k_\mu = 1.5$, $\mu = 2$, and $M_i = \mathrm{I}_2$, $i = 1, 2, 3, 4$. The initial states of the HMAS are randomly generated within the range of -5 to 5. The initial states of the distributed observers are given as $\mathbf{0}_3$.

The simulation results are presented in Figs. 2–5. The output trajectories of the closed-loop HMAS are given in Fig. 2. Within this figure, the output of the nonautonomous leader is indicated by a red pentagram, and the outputs of four followers are represented by square markers. From Fig. 2, it can be observed that the followers can form a quadrilateral formation and track the trajectory provided by the leader. The distributed observer error and the fixed-time TVF tracking errors are given in Figs. 3 and 4, respectively. From Fig. 4, it is not that the fixed-time TVF tracking errors can converge to the residual set $\{e_{yi}(t) | \|e_{yi}(t)\| \leq 0.05, i = 1, 2, 3, 4\}$ in 5 s. The norms of the control inputs of the HMAS are shown in Fig. 5. As a comparison, Fig. 6 illustrates the TVF tracking errors obtained through the utilization of the asymptotic controller proposed in [22]. It is worth noting that the initial conditions for both

Authorized licensed use limited to: Hong Kong Polytechnic University. Downloaded on September 15,2025 at 15:32:38 UTC from IEEE Xplore. Restrictions apply.

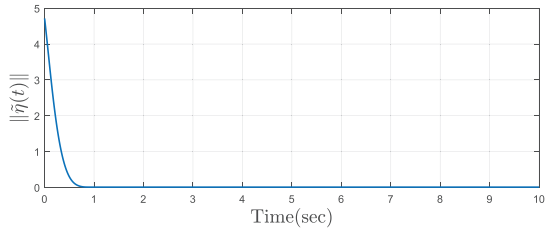

Fig. 3. Estimation error of the distributed state observer for Example 1.

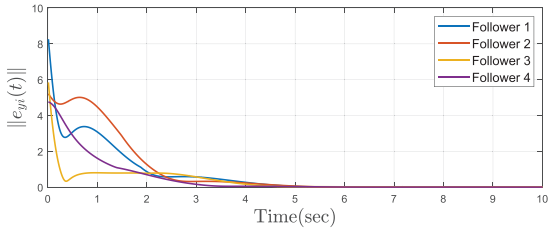

Fig. 4. TVF tracking errors with the fixed-time controller for Example 1.

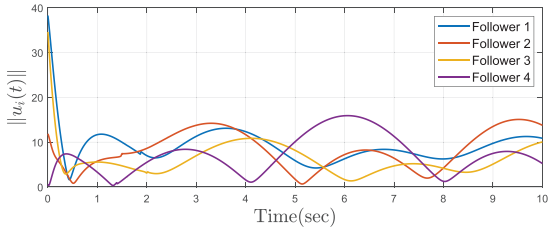

Fig. 5. Control inputs of the followers for Example 1.

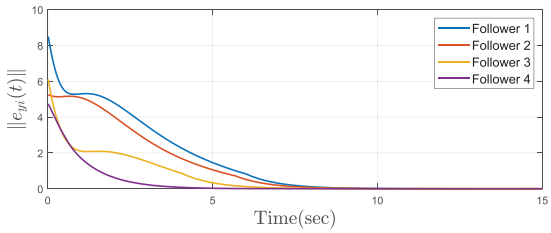

Fig. 6. TVF tracking errors with the asymptotic controller.

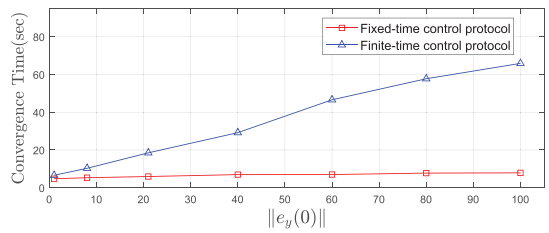

Fig. 7. Convergence time for different initial values in a wide range.

the HMAS and the distributed fixed-time observers are set to be identical in this comparison. It is evident from Figs. 4 to 6 that the fixed-time controller achieves a faster error convergence than the asymptotic controller.

In addition, we conduct a comparison between the fixed-time control protocol and the finite-time control protocol proposed in [26]. Fig. 7 shows the respective convergence times to the same residual set $\{e_{yi}(t)|\|e_{yi}(t)\| \leq 0.05,\ i = 1, 2, 3, 4\}$ across various initial states. As observed in Fig. 7, the convergence time based on the fixed-time control protocol remains small and well within the upper bound across a range of initial conditions, in contrast to that for the finite-time control protocol where it exhibits significant variations in response to different initial values. Figs. 8 and 9 show the transient responses of the TVF tracking errors obtained through the fixed-time and finite-time control protocols for one particular initial condition, respectively. Figs. 8 and 9 show that the fixed-time controller achieves a much faster error convergence than the finite-time controller.

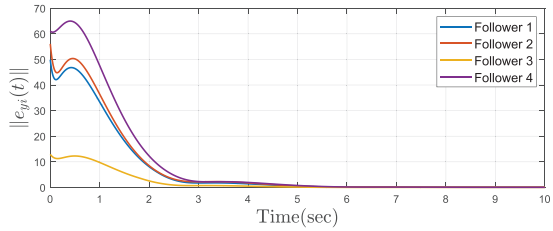

Fig. 8. TVF tracking errors with the fixed-time controller under the initial value $\|e_y(0)\| = 100$.

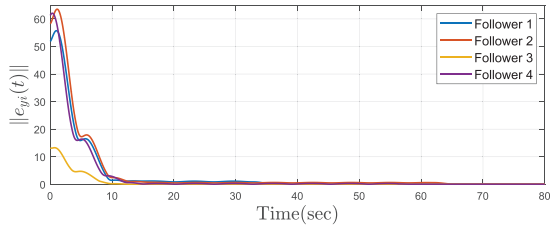

Fig. 9. TVF tracking errors with the finite-time controller under the initial value $\|e_y(0)\| = 100$.

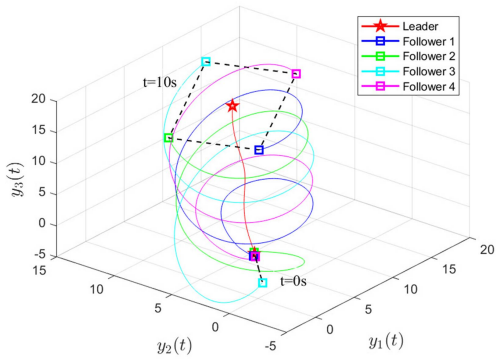

Fig. 10. Output trajectories of the HMAS for Example 2.

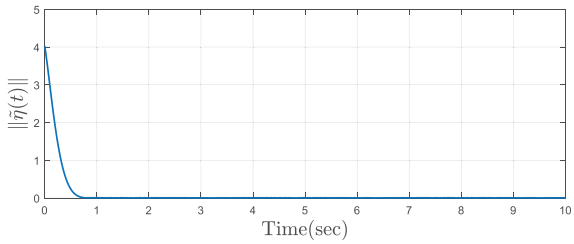

Fig. 11. Estimation error of the distributed state observer for Example 2.

Authorized licensed use limited to: Hong Kong Polytechnic University. Downloaded on September 15,2025 at 15:32:38 UTC from IEEE Xplore. Restrictions apply.

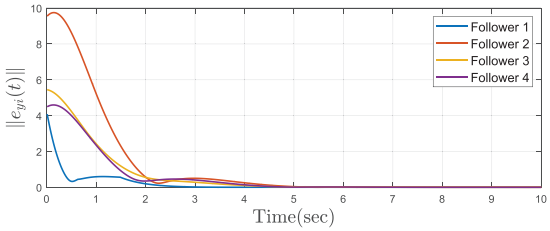

Fig. 12. TVF tracking errors for Example 2.

Example 2: Consider a group of HMAS consisting of different agents with heterogeneous dynamics in dimensions and parameters. The system matrices of the followers borrowed from [24] are given as

$$A_1 = \mathbf{0}_{3\times 3}, B_1 = \mathrm{I}_3, C_1 = \mathrm{I}_3$$

$$A_2 = \mathrm{I}_3 \otimes \begin{pmatrix} 0 & 1 \\ -2 & -2 \end{pmatrix}, B_2 = \mathrm{I}_3 \otimes \begin{pmatrix} 0 \\ -2 \end{pmatrix}, C_2 = \mathrm{I}_3 \otimes \begin{pmatrix} 1 & 0 \end{pmatrix}$$

$$A_3 = \mathrm{I}_3 \otimes \begin{pmatrix} 0 & 1 \\ -3 & -3 \end{pmatrix}, B_3 = \mathrm{I}_3 \otimes \begin{pmatrix} 0 \\ -2 \end{pmatrix}, C_3 = \mathrm{I}_3 \otimes \begin{pmatrix} 1 & 0 \end{pmatrix}$$

$$A_4 = \mathrm{I}_3 \otimes \begin{pmatrix} 0 & 1 & 0 \\ 0 & 0 & 1 \\ 1 & 2 & 1 \end{pmatrix}, B_4 = \mathrm{I}_3 \otimes \begin{pmatrix} 0 & 0 \\ 1 & 0 \\ 0 & 1 \end{pmatrix}, C_4 = \mathrm{I}_3 \otimes \begin{pmatrix} 1 & 0 & 0 \end{pmatrix}.$$

The system matrices of the leader are given as

$$A_0 = \mathrm{I}_3 \otimes \begin{pmatrix} 0 & 1 \\ 0 & 0 \end{pmatrix}, B_0 = \mathrm{I}_3 \otimes \begin{pmatrix} 0 \\ 1 \end{pmatrix}, C_0 = \mathrm{I}_3 \otimes \begin{pmatrix} 1 & 0 \end{pmatrix}.$$

The command input is given as $u_0(t) = [0.2\sin(t) 0.2\cos(t)\ 0.2\sin(t)]^\top$ and $\|u_0(t)\|_\infty \le \gamma = 0.2$.

The TVF vector $h_{xi}(t) = \begin{pmatrix} h_{xi}^1(t) \\ h_{xi}^2(t) \\ h_{xi}^3(t) \end{pmatrix}$ is specified by

$$h_{xi}^1 = h_{xi}^3 = \begin{pmatrix} r\sin(t + (i-1)\pi/2) \\ r\cos(t + (i-1)\pi/2) \end{pmatrix}$$

$$h_{xi}^2 = \begin{pmatrix} r\cos(t + (i-1)\pi/2) \\ -r\sin(t + (i-1)\pi/2) \end{pmatrix}, \quad i = 1, 2, 3, 4$$

and $h_{yi}(t) = [r\sin(t + (i-1)\pi/2)\ r\cos(t + (i-1)\pi/2)\ r\sin(t + (i-1)\pi/2)]^\top$ with $r = 5$.

For the desired formation $h_{yi}(t)$ generated by (3), choose $X_{h1} = \mathrm{I}_3 \otimes (1\ \ 0)$, $U_{h1} = \mathrm{I}_3 \otimes (0\ \ 1)$, $X_{h2} = \mathrm{I}_3 \otimes \begin{pmatrix} 1 & 0 \\ 0 & 1 \end{pmatrix}$, $U_{h2} = \mathrm{I}_3 \otimes (-\frac{1}{2}\ \ -1)$, $X_{h3} = \mathrm{I}_3 \otimes \begin{pmatrix} 1 & 0 \\ 0 & 1 \end{pmatrix}$, $U_{h3} = \mathrm{I}_3 \otimes (-\frac{2}{3}\ \ -1)$, $X_{h4} = \mathrm{I}_3 \otimes \begin{pmatrix} 1 & 0 \\ 0 & 1 \\ 0 & 0 \end{pmatrix}$, and $U_{h4} = \mathrm{I}_3 \otimes \begin{pmatrix} -1 & 0 \\ -1 & 2 \end{pmatrix}$ such that (6) holds. Solving (5) and (7) yields $X_1 = \mathrm{I}_3 \otimes (1\ \ 0)$, $U_1 = \mathrm{I}_3 \otimes (0\ \ 1)$, $X_2 = X_3 = \mathrm{I}_3 \otimes \begin{pmatrix} 1 & 0 \\ 0 & 1 \end{pmatrix}$, $U_2 = U_3 = \mathrm{I}_3 \otimes (-1\ \ -1)$, $X_4 = \mathrm{I}_3 \otimes \begin{pmatrix} 1 & 0 \\ 0 & 1 \\ 0 & 0 \end{pmatrix}$, $U_4 = \mathrm{I}_3 \otimes \begin{pmatrix} 0 & 0 \\ -1 & -2 \end{pmatrix}$, $R_1 = \mathbf{0}_{3\times 3}$, $R_2 = -\mathrm{I}_3 \otimes \frac{1}{2}$, $R_2 = -\mathrm{I}_3 \otimes \frac{1}{3}$, and $R_4 = \mathrm{I}_3 \otimes \begin{pmatrix} 1 \\ 0 \end{pmatrix}$.

The parameters in the distributed fixed-time observer (8) and controller (40) are given as $c_1 = 7$, $c_2 = 5$, $c_3 = 6$, $\alpha = 7/9$, $\beta = 907/700$, $\rho = 0.3$, $\bar{\gamma}_i = 1.2$, $k_\mu = 1.5$, $\mu = 2$, $M_1 = \mathrm{I}_3$, $M_2 = \mathrm{I}_6$, $M_3 = \mathrm{I}_6$, and $M_4 = \mathrm{I}_9$. The initial states of the HMAS are randomly generated within the range of -5 to 5. The initial states of the distributed observers are given as $\mathbf{0}_6$.

The simulation results are presented in Figs. 10–12. Fig. 10 shows that the outputs of the four followers achieve a 3-D quadrilateral and also track the output of the nonautonomous leader in a fixed time. Figs. 11 and 12 show the responses of the distributed observer error and TVF tracking errors, respectively. It can be observed that the fixed-time TVF tracking is achieved for the HMAS via the proposed control method.

V. Conclusion

This article has investigated the fixed-time TVF tracking control problem for HMASs with a nonautonomous leader. First, the fixed-time distributed observer is introduced to estimate the state of the nonautonomous leader within a fixed time. Then, unlike most existing methods, the fixed-time observer-based TVF tracking control protocol is put forward without a restrictive assumption, the full column rank of the input matrix. In addition, the convergence of the distributed observer errors and the TVF tracking errors have been analyzed. Simulations with comparisons have been conducted to demonstrate the effectiveness of the proposed controller. It is interesting to extend the proposed fixed-time TVF tracking approach to alleviate the problem of conservatism of upper bound on settling time in future work. Moreover, designing a distributed fixed-time control protocol that does not require the system matrices of the leader to be available to all followers is also meaningful.

Appendix

Lemma 3 (See [48]): For any $\iota_i \in \mathbb{R}$, $i = 1, 2, \ldots, n$, and any $p \in (0, 1]$, $(\sum_{i=1}^n |\iota_i|)^p \le \sum_{i=1}^n |\iota_i|^p \le n^{1-p}(\sum_{i=1}^n |\iota_i|)^p$. For any $p > 1$, $\sum_{i=1}^n |\iota_i|^p \le (\sum_{i=1}^n |\iota_i|)^p \le n^{p-1}\sum_{i=1}^n |\iota_i|^p$.

Lemma 4 (See [34]): Consider the system with dynamics described by $\dot{x} = g(x, t)$, where $g : \mathbb{R}^n \times [0, \infty) \to \mathbb{R}^n$ is a continuous vector function that satisfies $g(0, t) = 0$. Suppose there is a continuous, positive definite function $W(x) : \mathbb{R}^n \to \mathbb{R}$ such that $\dot{W}(x) \le -c_0(W(x))^c - d_0(W(x))^d$ for all $x \in \mathbb{R}^n$, where $c_0 > 0$, $d_0 > 0$, $0 < c < 1$, and $d > 1$. Then, the system is fixed-time stable, with an upper bound of the settling time given by $t \le \frac{1}{c_0(1-c)} + \frac{1}{d_0(d-1)}$.

Lemma 5 (See [49]): For a linear system

$$\dot{x}(t) = Ax(t) + Bu(t) \tag{60}$$

where $x \in \mathbb{R}^n$, $u \in \mathbb{R}^m$, and A and B are the system matrices.

If (A, B) is controllable and the rank of B is m, there exist a linear coordinate transformation $\xi(t) = Tx(t) \in \mathbb{R}^n$ such that $\xi(t) = [\xi_1^\top(t), \ldots, \xi_m^\top(t)]^\top$. Let ρ_i, $i = 1, \ldots, m$, be the controllability index of $\xi(t)$. Then, $\xi(t)$ can be described by $\xi(t) = \left[\xi_{1,1}(t), \ldots, \xi_{1,\rho_1}(t) \middle| \cdots \middle| \xi_{m,1}(t), \ldots, \xi_{m,\rho_m}(t)\right]^\top$ and

Authorized licensed use limited to: Hong Kong Polytechnic University. Downloaded on September 15,2025 at 15:32:38 UTC from IEEE Xplore. Restrictions apply.

the dynamics of $\xi_i(t)$, $i = 1, \ldots, m$, has the following form:

$$\begin{cases} \dot{\xi}_{i,1}(t) = \xi_{i,2}(t) \\ \dot{\xi}_{i,2}(t) = \xi_{i,3}(t) \\ \vdots \\ \dot{\xi}_{i,\rho_i}(t) = t_i^\top A^{\rho_i}\xi(t) + t_i^\top A^{\rho_i - 1}Bu(t) \end{cases}$$

where $t_i^\top = i_{r_i}^\top T$, $i_k \in \mathbb{R}^n$ is a vector with the k-th element being set to 1 and all the other elements being set to 0, and $r_i = \sum_{k=0}^{i-1}(1+\rho_k)$ with $\rho_0 = 0$.

Moreover, define $\xi^\rho(t) = [\xi_{1,\rho_1}(t), \ldots, \xi_{m,\rho_m}(t)]^\top \in \mathbb{R}^m$, one has

$$\dot{\xi}^\rho(t) = G\xi(t) + Mu(t) \tag{61}$$

where $G = \begin{pmatrix} t_1^\top A^{\rho_1} \\ \vdots \\ t_m^\top A^{\rho_m} \end{pmatrix}$ and $M = \begin{pmatrix} t_1^\top A^{\rho_1 - 1}B \\ \vdots \\ t_m^\top A^{\rho_m - 1}B \end{pmatrix}$ with M being invertible.

Lemma 6 (See [50]): Consider a system that is modeled as an nth order integrator

$$\begin{cases} \dot{x}_1(t) = x_2(t) \\ \dot{x}_2(t) = x_3(t) \\ \vdots \\ \dot{x}_n(t) = u(t) \end{cases} \tag{62}$$

where $x(t) = [x_1(t), \ldots, x_n(t)]^\top$ and $u(t)$ represent the state and control input, respectively.

The fixed-time stabilization control input is proposed as

$$u(t) = -\sum_{i=1}^{n} \left(\kappa_i \mathrm{sig}^{\alpha_i}(x_i(t)) + \bar{\kappa}_i \mathrm{sig}^{\beta_i}(x_i(t))\right) \tag{63}$$

where κ_i and $\bar{\kappa}_i$, $i = 1, \ldots, n$, are the positive constants satisfying the polynomials $s^n + \kappa_n s^{n-1} + \cdots + \kappa_2 s + \kappa_1$, and $s^n + \bar{\kappa}_n s^{n-1} + \cdots + \bar{\kappa}_2 s + \bar{\kappa}_1$ are Hurwitz. The values $\alpha_1, \ldots, \alpha_n$ and $\beta_1, \ldots, \beta_n$ can be chosen such that

$$\alpha_{i-1} = \frac{\alpha_i \alpha_{i+1}}{2\alpha_{i+1} - \alpha_i}$$

$$\beta_{i-1} = \frac{\beta_i \beta_{i+1}}{2\beta_{i+1} - \beta_i}$$

where $i = 1, 2, \ldots, n$, $\alpha_{n+1} = \beta_{n+1} = 1$, $\alpha_n = \alpha \in (1-\epsilon, 1)$, and $\beta_n = \beta \in (1, 1+\bar{\epsilon})$ for sufficiently small $\epsilon, \bar{\epsilon} > 0$.

Moreover, the settling time is bounded by

$$T_c \leq \frac{p\lambda_{\max}(P_1)}{(1-p)\lambda_{\min}(Q_1)}\lambda_{\max}^{\frac{1-p}{p}}(P_1) + \frac{q\lambda_{\max}(P_2)}{(q-1)\lambda_{\min}(Q_2)}\lambda_{\max}^{\frac{q-1}{q}}(P_2) \tag{64}$$

where P_i, $i = 1, 2$, are real symmetric positive definite matrices that satisfy the Lyapunov equation $P_i A_i + A_i^\top P_i = -Q_i$, with Q_i being an arbitrary positive definite matrix. The matrices A_i, $i = 1, 2$, have the following forms:

$$A_1 = \begin{pmatrix} 0 & 1 & \cdots & 0 \\ \vdots & \vdots & \ddots & \vdots \\ 0 & 0 & \cdots & 1 \\ -\kappa_1 & -\kappa_2 & \cdots & -\kappa_n \end{pmatrix}$$

$$A_2 = \begin{pmatrix} 0 & 1 & \cdots & 0 \\ \vdots & \vdots & \ddots & \vdots \\ 0 & 0 & \cdots & 1 \\ -\bar{\kappa}_1 & -\bar{\kappa}_2 & \cdots & -\bar{\kappa}_n \end{pmatrix}.$$

REFERENCES

[1] R. Olfati-Saber and R. M. Murray, "Distributed cooperative control of multiple vehicle formations using structural potential functions," *IFAC Proc. Volumes*, vol. 35, no. 1, pp. 495–500, 2002.

[2] R. Olfati Saber and R. M. Murray, "Consensus problems in networks of agents with switching topology and time-delays," *IEEE Trans. Autom. Control*, vol. 49, no. 9, pp. 1520–1533, Sep. 2004.

[3] J. Xu, Z. Wang, and Z. Jin, "Robust formation control for PWM-controlled mobile autonomous multi-agent systems," *IEEE Trans. Control Netw. Syst.*, vol. 11, no. 2, pp. 731–742, Jun. 2024.

[4] Y. Huang, Z. Meng, and D. V. Dimarogonas, "Prescribed performance formation control for second-order multi-agent systems with connectivity and collision constraints," *Automatica*, vol. 160, 2024, Art. no. 111412.

[5] W. Ren and R. W. Beard, "Decentralized scheme for spacecraft formation flying via the virtual structure approach," *J. Guidance, Control, Dyn.*, vol. 27, no. 1, pp. 73–82, 2004.

[6] I. Jeon, J. Lee, and M. Tahk, "Homing guidance law for cooperative attack of multiple missiles," *J. Guidance, Control, Dyn.*, vol. 33, no. 1, pp. 275–280, 2010.

[7] J. Yu, X. Dong, Q. Li, J. Lü, and Z. Ren, "Fully adaptive practical time-varying output formation tracking for high-order nonlinear stochastic multi-agent system with multiple leaders," *IEEE Trans. Cybern.*, vol. 51, no. 4, pp. 2265–2277, Apr. 2021.

[8] R. Huang, Z. Ding, and Z. Cao, "Distributed output feedback consensus control of networked homogeneous systems with large unknown actuator and sensor delays," *Automatica*, vol. 122, 2020, Art. no. 109249.

[9] F. Nemati, S. M. S. Hamami, and A. Zemouche, "A nonlinear observer-based approach to fault detection, isolation and estimation for satellite formation flight application," *Automatica*, vol. 107, pp. 474–482, 2019.

[10] X. Liu, F. Deng, W. Wei, and F. Wan, "Formation tracking control of networked systems with time-varying delays and sampling under fixed and Markovian switching topology," *IEEE Trans. Control Netw. Syst.*, vol. 9, no. 2, pp. 601–612, Jun. 2022.

[11] W. Ren, "Consensus strategies for cooperative control of vehicle formations," *IET Control Theory Appl.*, vol. 1, no. 2, pp. 505–512, 2007.

[12] J. A. Fax and R. M. Murray, "Information flow and cooperative control of vehicle formations," *IEEE Trans. Autom. Control*, vol. 49, no. 9, pp. 1465–1476, Sep. 2004.

[13] W. Ren and R. W. Beard, "Consensus seeking in multiagent systems under dynamically changing interaction topologies," *IEEE Trans. Autom. Control*, vol. 50, no. 5, pp. 655–661, May 2005.

[14] J. G. Romero, E. Nuño, E. Restrepo, and I. Sarras, "Global consensus-based formation control of nonholonomic mobile robots with time-varying delays and without velocity measurements," *IEEE Trans. Autom. Control*, vol. 69, no. 1, pp. 355–362, Jan. 2024.

[15] Y. Liu and Z. Liu, "Distributed adaptive formation control of multi-agent systems with measurement noises," *Automatica*, vol. 150, 2023, Art. no. 110857.

[16] Q. Van Tran, "Formation tracking control of heterogeneous underactuated planar agents with stable internal dynamics," in *Proc. IEEE 62nd Conf. Decis. Control*, 2023, pp. 5153–5158.

[17] M. Porfiri, D. G. Roberson, and D. J. Stilwell, "Tracking and formation control of multiple autonomous agents: A two-level consensus approach," *Automatica*, vol. 43, no. 8, pp. 1318–1328, 2007.

[18] W. Ren and N. Sorensen, "Distributed coordination architecture for multi-robot formation control," *Robot. Auton. Syst.*, vol. 56, no. 4, pp. 324–333, 2008.

Authorized licensed use limited to: Hong Kong Polytechnic University. Downloaded on September 15,2025 at 15:32:38 UTC from IEEE Xplore. Restrictions apply.

[19] X. Dong and G. Hu, "Time-varying formation tracking for linear multiagent systems with multiple leaders," *IEEE Trans. Autom. Control*, vol. 62, no. 7, pp. 3658–3664, Jul. 2017.
[20] F. A. Yaghmaie, R. Su, F. L. Lewis, and L. Xie, "Multiparty consensus of linear heterogeneous multiagent systems," *IEEE Trans. Autom. Control*, vol. 62, no. 11, pp. 5578–5589, Nov. 2017.
[21] Y. Shi, X. Dong, Y. Hua, J. Yu, and Z. Ren, "Distributed output formation tracking control of heterogeneous multi-agent systems using reinforcement learning," *ISA Trans.*, vol. 138, pp. 318–328, 2023.
[22] Y. Hua, X. Dong, G. Hu, Q. Li, and Z. Ren, "Distributed time-varying output formation tracking for heterogeneous linear multi-agent systems with a nonautonomous leader of unknown input," *IEEE Trans. Autom. Control*, vol. 64, no. 10, pp. 4292–4299, Oct. 2019.
[23] W. Song, J. Feng, H. Zhang, and Y. Cai, "Formation tracking control for heterogeneous multiagent systems with multiple nonautonomous leaders via dynamic event-triggered mechanisms," *IEEE Trans. Cybern.*, vol. 53, no. 11, pp. 7224–7237, Nov. 2023.
[24] Y. Hua, X. Dong, Q. Li, and Z. Ren, "Distributed adaptive formation tracking for heterogeneous multiagent systems with multiple nonidentical leaders and without well-informed follower," *Int. J. Robust Nonlinear Control*, vol. 30, no. 6, pp. 2131–2151, Nov. 2020.
[25] L. Wang and F. Xiao, "Finite-time consensus problems for networks of dynamic agents," *IEEE Trans. Autom. Control*, vol. 55, no. 4, pp. 950–955, Apr. 2010.
[26] J. Fu and J. Wang, "Observer-based finite-time coordinated tracking for general linear multi-agent systems," *Automatica*, vol. 66, pp. 231–237, 2016.
[27] G. Xiao, J. Wang, and D. Meng, "Adaptive finite-time consensus for stochastic multiagent systems with uncertain actuator faults," *IEEE Trans. Control Netw. Syst.*, vol. 10, no. 4, pp. 1899–1912, Dec. 2023.
[28] X. Shi, G. Wen, J. Cao, and X. Yu, "Finite-time distributed average tracking for multi-agent optimization with bounded inputs," *IEEE Trans. Autom. Control*, vol. 68, no. 8, pp. 4948–4955, Aug. 2023.
[29] R. Nie, W. Du, Z. Li, and S. He, "Finite-time consensus control for MASs under hidden Markov model mechanism," *IEEE Trans. Autom. Control*, vol. 69, no. 7, pp. 4726–4733, Jul. 2024.
[30] F. Xiao, L. Wang, J. Chen, and Y. Gao, "Finite-time formation control for multi-agent systems," *Automatica*, vol. 45, no. 11, pp. 2605–2611, 2009.
[31] Q. Wang, Y. Hua, X. Dong, P. Shu, J. Lü, and Z. Ren, "Finite-time time-varying formation tracking for heterogeneous nonlinear multiagent systems using adaptive output regulation," *IEEE Trans. Cybern.*, vol. 54, no. 4, pp. 2460–2471, Apr. 2024.
[32] J. Duan, H. Zhang, Y. Cai, and K. Zhang, "Finite-time time-varying output formation-tracking of heterogeneous linear multi-agent systems," *J. Franklin Inst.*, vol. 357, no. 2, pp. 926–941, 2020.
[33] P. Wang, C. Yu, and Y.-J. Pan, "Finite-time output feedback cooperative formation control for marine surface vessels with unknown actuator faults," *IEEE Trans. Control Netw. Syst.*, vol. 10, no. 2, pp. 887–899, Jun. 2023.
[34] A. Polyakov, "Nonlinear feedback design for fixed-time stabilization of linear control systems," *IEEE Trans. Autom. Control*, vol. 57, no. 8, pp. 2106–2110, Aug. 2012.
[35] Z. Zuo, "Nonsingular fixed-time consensus tracking for second-order multi-agent networks," *Automatica*, vol. 54, pp. 305–309, 2015.
[36] Z. Zuo, B. Tian, M. Defoort, and Z. Ding, "Fixed-time consensus tracking for multi-agent systems with high-order integrator dynamics," *IEEE Trans. Autom. Control*, vol. 63, no. 2, pp. 563–570, Feb. 2018.
[37] Y. Dong and Z. Chen, "Fixed-time synchronization of networked uncertain Euler–Lagrange systems," *Automatica*, vol. 146, 2022, Art. no. 110571.
[38] B. Ning, Q. Han, and Z. Zuo, "Practical fixed-time consensus for integrator-type multi-agent systems: A time base generator approach," *Automatica*, vol. 105, pp. 406–414, 2019.
[39] Y. Cai, H. Zhang, Y. Wang, Z. Gao, and Q. He, "Adaptive bipartite fixed-time time-varying output formation-containment tracking of heterogeneous linear multiagent systems," *IEEE Trans. Neural Netw. Learn. Syst.*, vol. 33, no. 9, pp. 4688–4698, Sep. 2022.
[40] W. Cheng, K. Zhang, B. Jiang, and S. X. Ding, "Fixed-time fault-tolerant formation control for heterogeneous multi-agent systems with parameter uncertainties and disturbances," *IEEE Trans. Circuits Syst. I: Reg. Papers*, vol. 68, no. 5, pp. 2121–2133, May 2021.
[41] W. Cheng, K. Zhang, and B. Jiang, "Distributed adaptive fixed-time fault-tolerant formation control for heterogeneous multiagent systems with a leader of unknown input," *IEEE Trans. Cybern.*, vol. 53, no. 11, pp. 7285–7294, Nov. 2023.
[42] D. Mellinger and V. Kumar, "Minimum snap trajectory generation and control for quadrotors," in *Proc. IEEE Int. Conf. Robot. Automat.*, 2011, pp. 2520–2525.
[43] Z. Qu, *Cooperative Control of Dynamical Systems: Applications to Autonomous Vehicles*. London, U.K.: Springer, 2009.
[44] J. Huang, *Nonlinear Output Regulation: Theory and Applications*. Philadelphia, PA, USA: Soc. Ind. Appl. Math., 2004.
[45] X. Dong, Y. Zhou, Z. Ren, and Y. Zhong, "Time-varying formation tracking for second-order multi-agent systems subjected to switching topologies with application to quadrotor formation flying," *IEEE Trans. Ind. Electron.*, vol. 64, no. 6, pp. 5014–5024, Jun. 2017.
[46] A. F. Filippov, *Differential Equations With Discontinuous Righthand Sides*. Dordrecht, The Netherlands: Springer, 2013.
[47] P. Wieland, R. Sepulchre, and F. Allgöwer, "An internal model principle is necessary and sufficient for linear output synchronization," *Automatica*, vol. 47, no. 5, pp. 1068–1074, 2011.
[48] G. H. Hardy, J. E. Littlewood, G. Pólya, and G. Pólya, *Inequalities*. Cambridge, U.K.: Cambridge Univ. Press, 1952.
[49] D. Luenberger, "Canonical forms for linear multivariable systems," *IEEE Trans. Autom. Control*, vol. TAC-12, no. 3, pp. 290–293, Jun. 1967.
[50] M. Basin, Y. Shtessel, and F. Aldukali, "Continuous finite-and fixed-time high-order regulators," *J. Franklin Inst.*, vol. 353, no. 18, pp. 5001–5012, 2016.

Shiyu Zhou (Graduate Student Member, IEEE) received the B.Eng. degree in automation from Northwestern Polytechnical University, Xi'an, China, in 2019, and the M.Eng. degree in control science and engineering from Beihang University, Beijing, China, in 2022. She is currently working toward the Ph.D. degree in control science and engineering with the Department of Biomedical Engineering, City University of Hong Kong, Hong Kong.

Her current research interests include cooperative control of multiagent systems and synchronization of complex networks.

Dong Sun (Fellow, IEEE) received the B.Eng. and M.Eng. degrees in precision instrument and mechanology from Tsinghua University, Beijing, China, in 1990 and 1994, respectively, and the Ph.D. degree in robotics and automation from The Chinese University of Hong Kong, Hong Kong, in 1997.

He is currently the Chair Professor with the Department of Biomedical Engineering, City University of Hong Kong.

Dr. Sun is currently a Fellow of the Canadian Academy of Engineering in Canada, Member of the European Academy of Sciences and Arts, Fellow of the International Academy of Medical and Biological Engineering, and Fellow of the American Society of Mechanical Engineers.

Gang Feng (Fellow, IEEE) received the Ph.D. degree in electrical engineering from the University of Melbourne, Melbourne, VIC, Australia, in 1992.

From 1992 to 1999, he was a Lecturer/Senior Lecturer with the School of Electrical Engineering, University of New South Wales at Sydney (UNSW Sydney), Sydney, NSW, Australia. Since 2000, he has been with the City University of Hong Kong, Hong Kong. He is currently the Chair Professor of mechatronic engineering with the City University of Hong Kong. His research interests include multiagent systems and control, intelligent systems and control, and networked systems and control.

Prof. Feng was the recipient of the Alexander von Humboldt Fellowship, the IEEE Transactions on Fuzzy Systems Outstanding Paper Award, the Changjiang Chair Professorship from the Education Ministry of China, and the CityU Outstanding Research Award. He is also an Associate Editor for *Journal of Systems Science and Complexity*, *Autonomous Intelligent Systems*, IEEE TRANSACTIONS ON AUTOMATIC CONTROL, IEEE TRANSACTIONS ON FUZZY SYSTEMS, IEEE TRANSACTIONS ON SYSTEMS, MAN, AND CYBERNETICS-PART C: APPLICATIONS AND REVIEWS, *Mechatronics*, and *Journal of Control Theory and Applications*. He is listed as an SCI Highly Cited Researcher by Clarivate Analytics. He is on the Advisory Board of Unmanned Systems.

Authorized licensed use limited to: Hong Kong Polytechnic University. Downloaded on September 15,2025 at 15:32:38 UTC from IEEE Xplore. Restrictions apply.